ChemPubSoc Europe

DOI: 10.1002/chem.201303792

CHEMISTRY
A European Journal
Full Paper

Rearrangement Reactions

Heavy-Atom Tunneling in the Ring Opening of a Strained Cyclopropene at Very Low Temperatures

Melanie Ertelt,[a] David A. Hrovat,[b] Weston Thatcher Borden,[b] and Wolfram Sander*[a]

Abstract: The highly strained 1H-bicyclo[3.1.0]-hexa-3,5-dien-2-one **1** is metastable, and rearranges to 4-oxacyclohexa-2,5-dienylidene **2** in inert gas matrices (neon, argon, krypton, xenon, and nitrogen) at temperatures as low as 3 K. The kinetics for this rearrangement show pronounced matrix effects, but in a given matrix, the reaction rate is independent of temperature between 3 and 20 K. This temperature independence means that the activation energy is zero in this temperature range, indicating that the reaction proceeds through quantum mechanical tunneling from the lowest vibrational level of the reactant. At temperatures above 20 K, the rate increases, resulting in curved Arrhenius plots that are also indicative of thermally activated tunneling. These experimental findings are supported by calculations performed at the CASSCF and CASPT2 levels by using the small-curvature tunneling (SCT) approximation.

Introduction

Quantum mechanical tunneling (QMT) is a fundamental phenomenon that is present in all chemical reactions.[1,2] It influences the kinetics of chemical reactions under conditions in which the QMT rates can compete with the rates of passage over, rather than through, the reaction barrier. Tunneling can become the dominant reaction mode at temperatures low enough that there is insufficient thermal energy to make passage over the barrier rapid. At very low temperatures, at which QMT occurs from the lowest vibrational level of the reactants, the reaction rate becomes independent of temperature, and if the probability of tunneling is small, the reaction rate has a very small Arrhenius pre-exponential factor. The tunneling probabilities depend strongly on the height and width of the barriers, so QMT is usually rapid only in reactions with small and narrow activation barriers. Matrix isolation spectroscopy is ideally suited for the investigation of tunneling reactions. Temperatures as low as 3 K can be obtained easily, precluding any thermally activated reactions, and kinetic studies can be run for long times of up to several weeks to monitor very slow reactions at extremely low temperatures.

In hydrogen-transfer reactions and CH insertions, QMT has been observed frequently,[3–14] whereas experimental evidence for tunneling involving heavier atoms or groups of atoms is still comparatively rare.[15–22] The bond shift in antiaromatic annulenes such as cyclobutadiene is one example for which calculations indicate that tunneling makes a considerable contribution to the rate constants even at higher temperatures.[23–25] Kinetic studies in low-temperature matrices reveal that the ring closure of some cyclobutanediyls is rather insensitive to temperature, which suggests a tunneling reaction mechanism.[16,26]

Another example of a reaction in which heavy-atom tunneling is implicated was published by us more than 20 years ago.[27] This is the rearrangement of the highly strained 1H-bicyclo[3.1.0]-hexa-3,5-dien-2-one **1** to 4-oxacyclohexa-2,5-dienylidene **2**. Cyclopropene **1** is formed through visible light photolysis at 10 K of the triplet carbene T-**2**, which is obtained easily through the photolysis of the matrix-isolated quinone diazide **3** (Scheme 1). The kinetics of the rearrangement were determined between 10 and 40 K in argon and several other matrices, and the half-life of **1** at 10 K was found to be of the order of seven days. Although the temperature range that could be used for kinetic measurements was limited, a curved

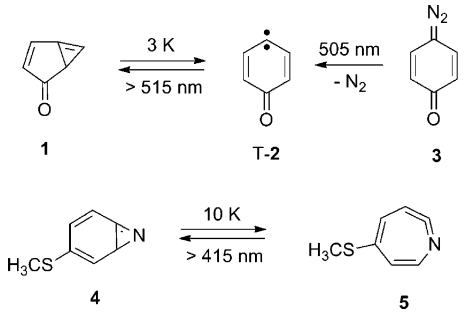

Scheme 1. Tunneling rearrangements of the strained cyclopropenes **1** and **4**.

[a] M. Ertelt, Prof. Dr. W. Sander
Lehrstuhl für Organische Chemie II
Ruhr-Universität Bochum, 44781 Bochum (Germany)
E-mail: wolfram.sander@rub.de

[b] Dr. D. A. Hrovat, Prof. Dr. W. T. Borden
Department of Chemistry and the
Center for Advanced, Scientific Computing and Modeling
University of North Texas
1155 Union Circle, #305070, Denton, Texas 76203-5070 (USA)

Supporting information for this article is available on the WWW under http://dx.doi.org/10.1002/chem.201303792.

Arrhenius plot with a zero activation barrier at temperatures below 20 K was observed, as expected for a tunneling reaction. However, it should be noted that curved Arrhenius plots do not necessarily result from tunneling.[28,29]

The ring opening of **1** to **2** is also a remarkable reaction, because **1** has a singlet ground state, whereas **2** is a triplet carbene. Thus, the **1**→**2** rearrangement requires an intersystem crossing (ISC) step. However, the position along the reaction coordinate connecting **1** to **T-2** at which ISC occurs could not be determined by these experiments.

The ring expansion of 1-methylcyclobutylfluorocarbene also shows unusual kinetic behavior.[17] The reaction rate increases only slightly between 8 and 25 K. The calculated activation barrier of 6.4 kcal mol^{-1} would not allow any thermal reaction in this temperature range, but the rate constant calculated for tunneling through this barrier was in excellent agreement with that measured at 8 K.

Recently, purely computational evidence was presented that the kinetics of the Bergman cyclization of a 10-membered enediyne is also influenced substantially by QMT, even at 37 °C.[30] In addition, experimental evidence indicates that the ring expansion of benzazirine **4** to cyclic ketenimine **5** at low temperatures also proceeds through QMT (Scheme 1).[22] Similarly to **1**, benzazirine **4** is a highly strained anti-Bredt cyclopropene that undergoes ring expansion readily. Thus, rearrangements of this type of compound may generally prove to be fruitful reactions for investigation in the search for molecules that react at low temperatures through heavy-atom tunneling.

With the advent of experimental and theoretical methods that were not available 20 years ago, when we initially discovered the rearrangement of **1** to **2**, we decided to use these advanced methods to reinvestigate this reaction. In particular, we are now able to perform experiments at temperatures down to 3 K, which, compared to 10 K, is more than a factor of three lower in *kT*. In addition, CASSCF and CASPT2 calculations can now be performed rapidly enough to generate potential energy surfaces, which can be used to compute tunneling rate constants for this reaction.

Results and Discussion

Matrix effects at 3 K

The kinetics of the **1**→**2** rearrangement were measured in solid neon, argon, krypton, xenon, and nitrogen at temperatures from 3 K to an upper temperature limited by the vapor pressure of the matrix (neon: 8 K; nitrogen: 35 K; argon: 40 K; krypton: 50 K; xenon: 65 K). The rearrangement is enhanced by the IR radiation from the light source of the IR spectrometer, so an IR band-pass filter blocking all IR light above 2000 cm^{-1} must be used to obtain meaningful kinetic data.

The decay and increase in intensity, respectively, of the strongest IR absorptions of **1** and **2** were monitored by IR spectroscopy. In all the matrices, the kinetics observed at 3 K matched those at 20 K very closely (neon matrices are usable only up to 8 K owing to the high vapor pressure of neon at higher temperatures). This temperature independence is a very strong indication that the rearrangement proceeds through QMT at these low temperatures. Rate constants that are independent of temperature over an absolute temperature range of more than 600% imply that the Arrhenius activation energy in this temperature range is essentially zero, as expected for a tunneling reaction that occurs from the lowest vibrational level of the reactant. At temperatures above 25 K, the rates increase rapidly, indicating that the tunneling reaction becomes thermally activated, and between 15 and 25 K, both the thermally activated and nonactivated tunneling reactions contribute to the overall rate. This observation is in excellent agreement with the conclusion drawn in our first publication, although at that time, we could only measure the rates above 10 K.[27]

Comparison of the kinetic data obtained at 3 K in different matrices reveals surprisingly strong matrix effects for the **1**→**2** rearrangement. In argon and neon, the rates are very similar, whereas in nitrogen, krypton, and xenon, the decay is markedly accelerated (Figure 1). Thus, different matrix hosts (xenon, krypton, argon, and nitrogen) result in different rates for the rearrangement of **1** to **2** under otherwise similar conditions. It appears that the matrix has a strong influence on the barrier width and height, leading to an acceleration of the tunneling rates in xenon compared to those in argon. In xenon at 3 K, the half-life of **1** is only about 5 h (compared with seven days in argon), which results in a rapid decrease in the concentration of **1** with time in a Xe matrix.

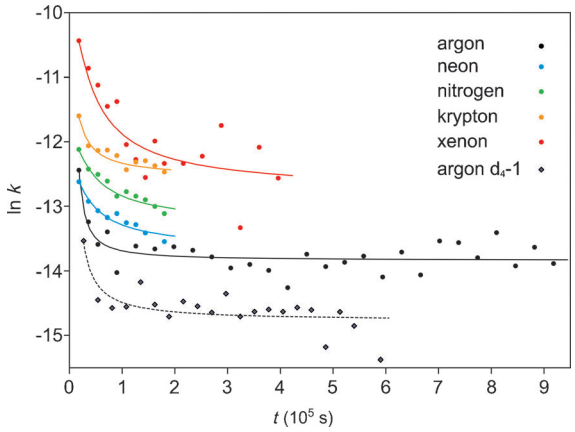

Figure 1. Rate constants *k* for the **1**→**2** rearrangement measured in various matrices at 3 K as a function of the measurement time.

The kinetic behavior of the **1**→**2** rearrangement is complicated, because the rate constant *k* measured in a given matrix at 3 K is not constant, but decreases over time (Figure 1). This is observed frequently in solid-state reactions resulting in dispersive kinetics. Some molecules of **1** are formed in "fast" matrix sites and rearrange much more quickly than others that occupy "slow" sites. Thus, instead of the clean first-order kinetics expected for unimolecular reactions in the gas phase, the observed rates depend not only on the temperature, but also on the time the experiments have been running, because "fast" sites react first and "slow" sites later.

The kinetics measurements were started directly after the formation of **1** through the irradiation of carbene **2**, and the decay of **1** and reformation of **2** were followed for several hours to several days (Figure 1). In a long-duration experiment in argon, the rate dropped from $4\times10^{-6}\,s^{-1}$ after 5 h to $1\times10^{-6}\,s^{-1}$ after two days, but remained constant after that time (the kinetics were followed for ten days at 3 K, Figure 1). The largest rate was observed in xenon, with $k>2\times10^{-5}$ at the beginning of the measurements, but this rate also showed the fastest decline over time. Owing to the rapidly decreasing concentration of **1** in xenon, the kinetics could only be followed for about four days.

A comparison of the changes in the rates measured in various matrices suggests that the rate constants converge to values close to $10^{-6}\,s^{-1}$, although there still seem to be significant differences between the different matrices (Figure 1). This kinetic behavior can be reproduced by using the same matrix several times. After the decay of **1** and formation of **2**, cyclopropene **1** is recovered upon subsequent irradiation of the matrix with visible light (>515 nm), and its decay can be monitored again.

Nonexponential decays have been observed for many unimolecular reactions that are influenced by their microenvironment. In particular, reactions in solid matrices[31] and also different processes such as protein folding[32] or DNA duplex dissociation[33] often show a decrease in rate constants over time, and thus, nonexponential decay. However, most of these reactions proceed thermally, rather than through QMT as in the **1**→**2** rearrangement.

An important question concerns how the environment influences QMT.[31,34–36] In the **1**→**2** rearrangement, the slowest tunneling rates and the lowest overall drops in the rate constants are observed for the least interacting rare gases, that is, neon and argon. The fastest rates and largest drops in rate constants are both found in xenon, the strongest interacting rare gas. It is tempting to assume that, depending on the matrix site in which cyclopropene **1** is trapped, individual matrix atoms interact more or less strongly with **1**. Molecules of **1** trapped in strongly interacting matrix sites rearrange first, leaving unreacted molecules in less interacting sites behind. The weak interactions between the matrix and trapped species might depend on the polarity, polarizability, and other properties of the trapped species. ISC is necessary for the interconversion of singlet **1** to triplet **2**, so it is tempting to hypothesize that the heavy-atom effect of xenon increases the ISC rates. This increase could affect the overall rates for the **1**→**2** rearrangement if, in xenon, **1** tunnels directly to **T-2** rather than to **S-2**.

Arrhenius plots

The matrix effects leading to dispersed kinetics (see discussion above) make it difficult to extract physically meaningful rate constants from the kinetic data. Despite it being a unimolecular reaction, in the solid state, the kinetics of the **1**→**2** rearrangement cannot be described by a single rate constant k, but rather, a distribution of rate constants has to be considered to fit the experimental data. Siebrand and Wildman introduced the empirical exponent β to match the experimental data (stretched exponent method), as shown in Equation (1).

$$[X]_t = [X]_0 \cdot \exp(-(kt)^{\beta}) \qquad (1)$$

Without environmental effects, $\beta=1$ should be observed. In our experiments, we find that β lies in a range between 0.5 and 1, depending on the matrix, the temperature, and the time that we start measuring the kinetics after the generation of **1**. We used Equation (1) to fit the kinetic data of the **1**→**2** rearrangement and to extract meaningful rate constants from the complete set of data for a given temperature and matrix.

Using these data, we obtain curved Arrhenius plots in argon, xenon, and nitrogen, with the onset of temperature dependence in the rate constants occurring at around 20 K. A problem with the measurements in argon and nitrogen is that at temperatures above 30 and 25 K, respectively, these matrices become soft and start to sublime off the cold window. Therefore, the data measured at these higher temperatures are less reliable because of the deterioration of the matrix. In neon, the matrix evaporates rapidly even at 8 K. Xenon matrices, on the other hand, persist to much higher temperatures (up to 60 K).

In xenon, the transition between thermal activation and temperature-independent tunneling from the lowest vibrational level of the reactant is observed at a similar temperature to that in argon. This observation indicates that the curved Arrhenius plot comes not from a matrix effect, but rather, results from the intrinsic properties of the matrix-isolated molecules. The Arrhenius plots in Figure 2 show clearly that the fastest rate for the rearrangement occurs in xenon, with a slower rate in nitrogen, and the slowest rates in argon and neon.

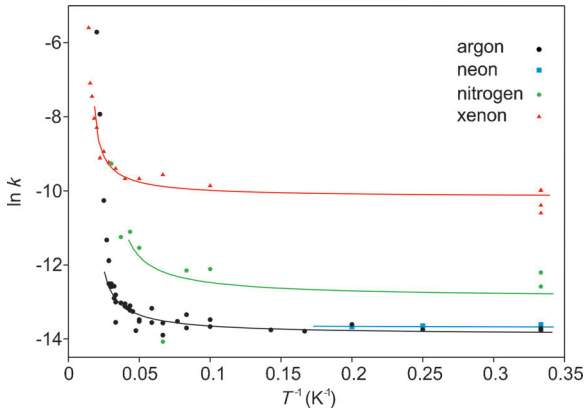

Figure 2. Arrhenius plots for the **1**→**2** rearrangement in neon, argon, xenon, and nitrogen.

Kinetic isotope effect

In the **1**→**2** rearrangement, no CH bond is broken, and thus, only a secondary kinetic isotope effect (KIE) is expected upon substitution of the H atoms in **1** by deuterium. For measurement of the KIE, the perdeuterated cyclopropene (**1**-d_4) was generated in argon matrices, and the rearrangement was followed at 3 K for up to seven days. The experiments were also

performed with an approximately 1:1 mixture of **1** and **1**-d_4 to ensure identical conditions. Deuteration results in a drop in the rates from $k_H = 1.2 \pm 0.1 \times 10^{-6}\ s^{-1}$ for **1** to $k_D < 2 \times 10^{-7}\ s^{-1}$ for **1**-d_4, which corresponds to an increase in half-life in Ar from 7 to over 45 days. The KIE is determined to be >6, and within the error limits of our rate measurements, is independent of temperature between 3 and 20 K.

However, owing to the very long half-life (several weeks) of the rearrangement of **1**-d_4, only a small fraction of the decay can be monitored, which introduces a large statistical error into the measurements. In addition, because the observed rates are larger at the beginning of the measurements and become constant only after a substantial fraction of decay has occurred, we expect that the observed reaction rate for **1**-d_4 is dominated by "fast" matrix sites, and is, thus, probably too large relative to the average rate of rearrangement of undeuterated **1**. Therefore, the actual KIE in the absence of such matrix effects in Ar is probably considerably larger than six. In fact, in xenon, a KIE of approximately 24 is measured, and this too could be a lower limit.

Calculations

The final product of the rearrangement of cyclopropene **1** is T-**2**, that is, the carbene in its triplet ground state. Thus, T-**2** must be lower in energy than **1**, and an ISC step has to occur somewhere along the reaction coordinate connecting **1** to T-**2**.

Electronic structure calculations at several different levels of theory have all indicated not only that **2** has a triplet ground state, but also that, perhaps surprisingly, the lowest singlet state of **2** (S-**2**) is the open-shell singlet state ($^1B_1$).[37–39] In the lowest singlet state of most carbenes, a pair of electrons occupies the σ MO on the carbene center. However, the open-shell singlet state S-**2** has the same orbital occupancy as the triplet T-**2**, with only one electron occupying the σ orbital and a second electron of opposite spin occupying the 2p-π MO.

A reasonable mechanism for the formation of T-**2** from **1** at cryogenic temperatures is ring opening of **1** to S-**2** occurring through QMT, followed by ISC of S-**2** to T-**2.** This mechanism requires that a) S-**2** and T-**2** both be lower in energy than **1,** and b) QMT from **1** to S-**2** occurs with a rate constant of about $10^{-6}\ s^{-1}$. Both of these mechanistic postulates were tested computationally.

Computational methodology

We performed (8/8)CASSCF and CASPT2[40] calculations of a) the relative energies of **1**, S-**2**, and T-**2**, and b) the rate constant for ring opening of **1** to S-**2** through QMT. The tunneling calculations were performed using variational transition state theory (VTST)[41] and the small-curvature tunneling (SCT) approximation.[42]

VTST + SCT rate calculations, performed in conjunction with B3LYP energy and derivative evaluations, have given rate constants that are in excellent agreement with those measured around 8 K for the ring expansion reactions of 1-methylcyclobutylfluorocarbene[17] and noradamantylchlorocarbene.[18,43] Calculations using the same methodology have provided ^{13}C kinetic isotope effects for the ring opening of the cyclopropylcarbinyl radical at low temperatures, which are also in excellent agreement with the experimental values.[20]

The open-shell nature of S-**2** made it impossible to use DFT to perform tunneling calculations, because DFT can describe triplets and closed-shell singlets correctly, but not open-shell singlets. Therefore, (8/8)CASSCF calculations were performed, using the 6-31G(d) basis set, to generate the potential energy surface connecting **1** to S-**2** and to calculate the CASSCF tunneling rates. In the computation of the CASPT2 tunneling rates, the (8/8)CASSCF energies of **1**, S-**2**, and the transition state connecting them were replaced with the CASPT2 energies of these stationary points. Tunneling calculations were then performed by using the interpolated single-point energy (VTST-ISPE) method.[44] The 6-31G(d), cc-pVDZ,[45] and cc-pVTZ basis sets[46] were used for the CASPT2 energy calculations.

The results of the (8/8)CASSCF and CASPT2 calculations served as the input for Polyrate,[47] which was used to compute the rate constants for the ring opening of **1** to S-**2** through QMT. The (8/8)CASSCF calculations were performed with Gaussian09,[48] using Gaussrate[49] as the interface between Gaussian09 and Polyrate. The CASPT2 energy calculations were carried out with MOLCAS 7.4.[50]

Computational results

Figure 3 shows the (8/8)CASSCF/6-31G(d) optimized geometries of **1**, S-**2**, T-**2**, and the transition structure connecting **1** to S-**2**. Reoptimization of these geometries at the CASPT2/6-31G(d) level of theory (see Figure S1 in the Supporting Information) resulted in bond-length changes of less than 0.02 Å and changes in the relative CASPT2 energies of less than 0.5 kcal mol^{-1}.

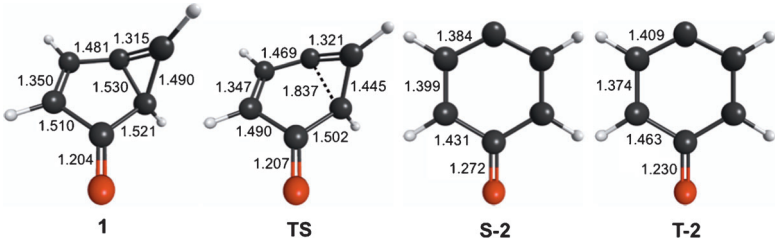

Figure 3. (8/8)CASSCF/6-31G(d) bond lengths [Å].

Although S-**2** and T-**2** each have one electron in the carbene σ orbital and another unpaired electron in the $3b_1$ π MO, Figure 3 shows that the geometries of these two states are

rather different. This is because the $3b_1$ MO in the triplet is very different from the $3b_1$ MO in the singlet.

In the triplet state, the Pauli exclusion principle prevents the unpaired σ and π electrons from appearing simultaneously in the region of space in which the σ and 2p-π AOs on the carbenic carbons overlap. Consequently, in the triplet state, the $3b_1$ π MO has a large coefficient on the carbene carbon. Indeed, the bond lengths in T-**2** suggest that its dominant resonance structure is that shown in Figure 3, with a strong π bond to oxygen and the unpaired electron in a pentadienyl-like nonbonding MO, with significant unpaired density in the carbene 2p-π AO.

In contrast, in the open-shell singlet state, the electrons in the σ and $3b_1$ π MOs have opposite spins, so the motions of these two electrons are actually anticorrelated in the regions of space where the σ and π AOs on the carbenic carbons overlap. Therefore, if the $3b_1$ π electron appears at the carbene carbon, there is a large Coulombic repulsion energy between this π electron and the electron of opposite spin in the σ orbital on this carbon. Consequently, unlike the case in the T-**2** state, in the S-**2** state, the $3b_1$ π MO has a very small coefficient on the carbene carbon. Indeed, the bond lengths in Figure 3 for S-**2** suggest a dominant resonance structure with the unpaired π electron localized largely in a 2p-π AO on the oxygen.

Although CASSCF calculations deal satisfactorily with static electron correlation, CASPT2 calculations also include the effects of dynamic correlation between electrons.[40] Consequently, CASPT2 is expected to give much more reliable relative energies than CASSCF. Figure 4 shows schematically the relative energies of **1**, S-**2**, and the transition structure that connects them at both the (8/8)CASSCF and CASPT2 levels of theory, using the 6-31G(d) basis set. Also shown is the relative energy of the triplet ground state of the product of ring opening (T-**2**) at both levels of theory.

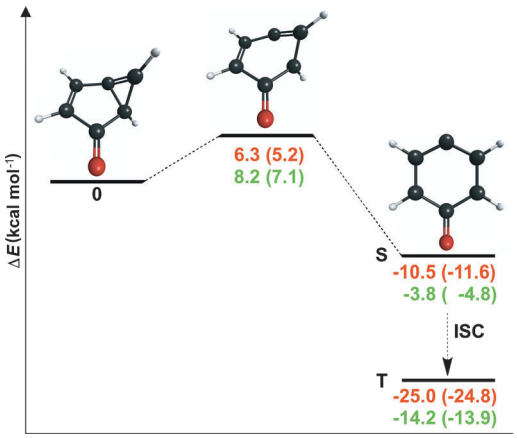

Figure 4. (8/8)CASSCF (red) and CASPT2 (green)/6-31G(d) relative energies [kcal mol^{-1}]. Zero-point energy corrected values are in parentheses.

(8/8)CASSCF and CASPT2 both predict that the ring opening of **1** to S-**2** is exothermic, and passes over a reaction barrier that is computed to be 1.9 kcal mol^{-1} higher at the CASPT2 than at the (8/8)CASSCF level of theory. The CASPT2 barrier is 8.2 kcal mol^{-1} (7.1 kcal mol^{-1} with ZPE corrections). Absorption of a photon of IR around 2000 cm^{-1} would deposit 5.7 kcal mol^{-1} in the matrix-isolated molecule. This amount of energy, although not enough to take **1** over the barrier, could allow **1** to tunnel to S-**2** closer to the top of the barrier, where the energy below the top of the barrier is smaller and the barrier is narrower than at the bottom of the barrier.

In addition to its higher barrier, the ring-opening reaction is computed to be 6.7 kcal mol^{-1} less exothermic at the CASPT2 than at the (8/8)CASSCF level of theory. The reason for the smaller reaction exothermicity at the CASPT2 level of theory is that CASPT2 correlates the electrons in all three of the strained σ bonds of the cyclopropene ring in **1,** whereas (8/8)CASSCF correlates the electrons only in the σ bond that is broken in the ring-opening reaction.

The lower exothermicity of the ring-opening reaction at the CASPT2 level of theory should make the height and width of the CASPT2 barrier greater than those of the CASSCF barrier. The heights and widths of the CASSCF and CASPT2 barriers are shown schematically in Figure 5, in which the barrier heights are plotted as a function of *S*, the progress (in arbitrary units) along the reaction coordinate.

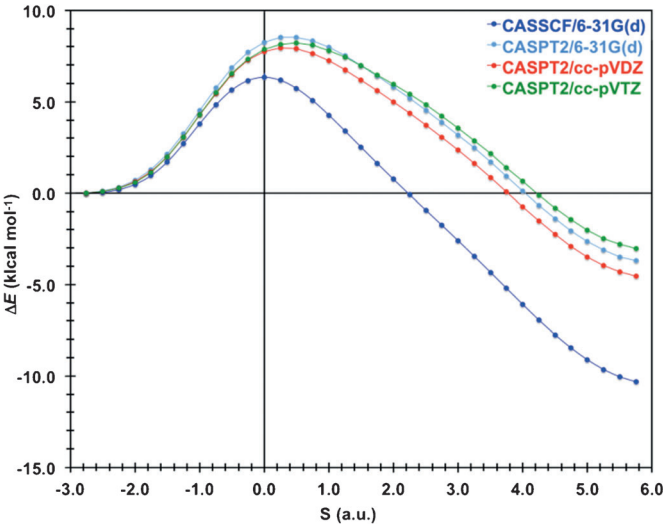

Figure 5. (8/8)CASSCF/6-31G(d) and interpolated single-point energy (ISPE) CASPT2 energy curves. The width of the barrier at its base is given by 3.0 plus the value of *S* at which each curve crosses the y axis.

Rate constants for tunneling reactions decrease exponentially with the product of the width of the barrier and the square root of the energy below the top of the reaction barrier at which tunneling occurs.[51] Consequently, tunneling rates are more sensitive to barrier width than to barrier height.[52,53] Thus, the greater height and especially the greater width of the CASPT2 barrier should both make the calculated rate constants for tunneling smaller at the CASPT2 than at the CASSCF level of theory.

Our calculations of the rates constants for ring opening of **1** to S-**2** show that the rate constants are independent of temperature below about 50 K (the calculated rate constants are

given as a function of temperature in Table S1 of the Supporting Information). Therefore, up to 50 K, tunneling occurs from the lowest vibrational level of the reactant without any contribution from tunneling from thermally populated, excited vibrational levels.

The temperature-independent (8/8)CASSCF and CASPT2 rate constants, computed with the 6-31G(d) basis set, are given in Table 1. The rate constants are calculated to be 66 s^{-1} and 2.3×10^{-8} s^{-1}, respectively. As expected, the CASPT2 rate constant is calculated to be much smaller than the CASSCF rate constant. However, the 3×10^{9} ratio of these two rate constants reveals how sensitive the rate constants for tunneling are to the differences in barrier heights and barrier widths that are shown schematically in Figure 5.

Table 1. Calculated and measured low-temperature rate constants (s^{-1}) for the ring opening of **1** to S-**2** and of **1**-d_4 to S-**2**-d_4.

Calculation	k_H (**1**→S-**2**)	k_D (**1**-d_4→S-**2**-d_4)	k_H/k_D
CASSCF/G[a]	6.6×10^{1}	1.3×10^{1}	5.1
CASPT2/G[a]	2.3×10^{-8}	4.4×10^{-11}	520
CASPT2/D[b]	2.4×10^{-6}	1.0×10^{-8}	240
CASPT2/T[c]	2.6×10^{-8}	2.2×10^{-11}	1200
experiment[d]	1.2×10^{-6}	$<2\times10^{-7}$	>6

[a] 6-31G(d) basis set. [b] cc-pVDZ basis set. [c] cc-pVTZ basis set. [d] Argon matrix.

Figure 5 shows that, not surprisingly, the CASPT2 barrier heights and widths depend on the basis set with which the calculations are performed. The cc-pVDZ basis set gives the lowest and narrowest barrier. The cc-pVTZ basis set gives a barrier that is only 0.1 kcal mol^{-1} higher than that computed with cc-pVDZ, but the transformation of **1** to S-**2** is calculated to be 1.6 kcal mol^{-1} less exothermic with cc-pVTZ than with cc-pVDZ. Consequently, as shown in Figure 5, the cc-pVTZ reaction barrier is not only slightly higher, but also wider than the cc-pVDZ barrier.

The 6-31G(d) reaction barrier is 0.4 kcal mol^{-1} higher than the cc-pVTZ barrier, but the calculated reaction exothermicity is 0.7 kcal mol^{-1} larger with the former basis set than with the latter. Therefore, as shown in Figure 5, the 6-31G(d) reaction barrier is calculated to be slightly narrower than the cc-pVTZ barrier.

As already noted, not only the barrier heights but also the barrier widths affect the calculated temperature-independent rate constants for tunneling from the lowest vibrational level of **1** to S-**2**. As shown in Table 1, the cc-pVDZ basis set, which gives a reaction barrier that is both lower and narrower than the cc-pVTZ and 6-31G(d) barriers, gives a CASPT2 rate constant about two orders of magnitude larger than those computed with the cc-pVTZ and 6-31G(d) basis sets. The CASPT2/cc-pVDZ temperature-independent rate constant of 2.4×10^{-6} s^{-1} is only a factor of two larger than the experimental value of 1.2×10^{-6} s^{-1} in argon, but this agreement is clearly fortuitous, because the larger cc-pVTZ basis set gives poorer agreement with the experimental rate constant.

Table 1 also gives the k_H/k_D kinetic isotope effects (KIEs) for the ring opening of **1** to S-**2** and **1**-d_4 to S-**2**-d_4. The tunneling rates decrease exponentially with the product of the barrier width, the square root of the energy below the top of the reaction barrier at which tunneling occurs, and the square root of the effective tunneling mass.[51] Wide and/or high barriers are responsible for the smallest rate constants for tunneling of **1** to S-**2** in Table 1, so it follows that the smallest calculated rate constants for the ring opening of undeuterated **1** in Table 1 should be associated with the largest KIEs. This is generally found to be the case.

Although the CASPT2 calculations give much better agreement with the experimental rate constant for the ring opening of undeuterated **1** than the (8/8)CASSCF calculations, it appears that the CASPT2 calculations may overestimate the size of the experimental KIE. Even the CASPT2/cc-pVDZ calculations, which give the calculated rate constant for the ring opening of **1** to S-**2** that is in the best agreement with the experimental result, overestimates by a factor of 40 the effect of deuterium on the rate of ring opening of **1**-d_4 to S-**2**-d_4. However, as noted in the section on the experimental determination of the kinetic isotope effect, the value of $k_H/k_D\approx6$ in an argon matrix is almost certainly a lower limit, and the actual size of the kinetic isotope effect could be considerably higher.

Conclusion

The ring opening of the highly strained cyclopropene **1** proceeds through QMT at temperatures as low as 3 K. The final product is the triplet ground-state carbene T-**2**, and therefore, an intersystem crossing (ISC) step is necessary during the rearrangement. This suggests that the primary product of the rearrangement is the singlet carbene S-**2**, which undergoes subsequent ISC to T-**2**.

Both (8/8)CASSCF and CASPT2 calculations predict an open-shell singlet state for the carbene S-**2**. At the more reliable CASPT2 level of theory, the activation energy for the ring opening of **1** to **S-2** is calculated to be 8 kcal mol^{-1}, and the energy of reaction is found to be −4 kcal mol^{-1}.

The reaction rates expected for the rearrangement **1** to **S-2** by passage over a reaction barrier of 6–8 kcal mol^{-1} at cryogenic temperatures are effectively zero. The fact that this rearrangement occurs at 3 K is therefore a very strong indication that this reaction proceeds by tunneling through the reaction barrier.

Between 3 and 20 K, the rate constants for this rearrangement are independent of temperature within the error limits of our measurements. Thus, the experimental activation energy is zero, as expected for a tunneling reaction. At higher temperatures, the rates increase, suggesting that thermally activated tunneling contributes to the rates. Argon and nitrogen matrices begin to soften at these higher temperatures, so the rates of rearrangement measured above 20 K may have contributions that involve changes in the matrix (e.g., rearrangements of the rare gas atoms surrounding matrix-isolated atoms of **1**, rotation of molecules of **1** in the matrix, etc.).

The results of our tunneling calculations are in reasonable agreement with our experimental results. Our calculations predict that tunneling dominates the reaction rates at temperatures below 50 K. Our CASPT2/cc-PVDZ calculations reproduce very closely the experimental rate of reaction of **1** in argon.

Unfortunately, the calculated CASPT2/cc-PVDZ KIE for the rearrangement of **1**-d_4 is about forty times larger than the experimental value measured in argon. However, the experimental value may contain large errors because of the extremely slow rate of rearrangement of **1**-d_4, and only a lower limit for the experimental value of k_H/k_D can actually be estimated. Therefore, the apparently sizable discrepancy between the experimental and calculated KIEs may reflect errors in both sets of values.

Experimental Section

Materials

4-Diazo-2,5-cyclohexadien-1-one **3** and (d_4)-4-diazo-2,5-cyclohexadien-1-one **(3**-d4) were synthesized according to literature procedures.

4-Diazo-2,5-cyclohexadien-1-one 3

IR (Ar, 3 K): $\tilde{\nu}$ = 1636 (vs), 1630 (vs), 1456 (w), 1407 (w), 1241 (s) 1146 (s) 1084 (vw), 845 (m), 792 (w), 775 (w), 718 cm^{-1} (m).

(d4)-4-Diazo-2,5-cyclohexadien-1-one (3-d4)

IR (Ar, 3 K): $\tilde{\nu}$ = 1620 (vs), 1562 (s), 1416 (w), 1305 (s), 1237 (w) 1191 (vw) 1140 (m), 830 (m), 814 (m), 745 (m), 658cm^{-1} (m).[6,8]

Matrix isolation

Matrix isolation experiments were performed by using a closed-cycle helium compressor (CSW-71, Sumitomo Heavy Industries Ltd) to cool a CsI spectroscopic window to 3 K. FTIR spectra were recorded on a Bruker Vertex 70v spectrometer with a resolution of 0.5 cm^{-1} by using a DLaTGs detector in the range 400–4000 cm^{-1}. For details see Supporting Information.

Acknowledgements

The research in Germany was supported by the Cluster of Excellence RESOLV (EXC 1069) funded by the Deutsche Forschungsgemeinschaft. The research in the U.S. was supported by Grant CHE-0910527 from the National Science Foundation and Grant B0027 from the Robert A. Welch Foundation.

Keywords: calculations · carbene · matrix isolation · rearrangement · tunneling

[1] K. U. Ingold in *Hydrogen-Transfer Reactions*, (Eds: J. T. Hynes, J. P. Klinman, H.-H. Limbach, R. L. Schowen), Wiley-VCH, Weinheim, **2007**, pp. 875 – 893, Chapter 28.
[2] H.-H. Limbach, K. B. Schowen, R. L. Schowen, *J. Phys. Org. Chem.* **2010**, *23*, 586 – 605.
[3] O. L. Chapman, J. W. Johnson, R. J. McMahon, P. R. West, *J. Am. Chem. Soc.* **1988**, *110*, 501 – 509.
[4] M. S. Platz, *Acc. Chem. Res.* **1988**, *21*, 236 – 242.
[5] E. J. Dix, M. S. Herman, J. L. Goodman, *J. Am. Chem. Soc.* **1993**, *115*, 10424 – 10425.
[6] P. Zuev, R. S. Sheridan, *J. Am. Chem. Soc.* **1994**, *116*, 4123 – 4124.
[7] P. S. Zuev, R. S. Sheridan, *J. Am. Chem. Soc.* **2001**, *123*, 12434 – 12435.
[8] T. V. Albu, B. J. Lynch, D. G. Truhlar, A. C. Goren, D. A. Hrovat, W. T. Borden, R. A. Moss, *J. Phys. Chem. A* **2002**, *106*, 5323 – 5338.
[9] H. Tomioka, *Springer Ser. At. Plasmas* **2004**, *36*, 147 – 172.
[10] D. Ley, D. Gerbig, J. P. Wagner, H. P. Reisenauer, P. R. Schreiner, *J. Am. Chem. Soc.* **2011**, *133*, 13614 – 13621.
[11] S. Wierlacher, W. Sander, M. T. H. Liu, *J. Am. Chem. Soc.* **1993**, *115*, 8943 – 8953.
[12] S. Henkel, Y. A. Huynh, P. Neuhaus, M. Winkler, W. Sander, *J. Am. Chem. Soc.* **2012**, *134*, 13204 – 13207.
[13] P. R. Schreiner, H. P. Reisenauer, D. Ley, D. Gerbig, C.-H. Wu, W. D. Allen, *Science* **2011**, *332*, 1300 – 1303.
[14] P. R. Schreiner, H. P. Reisenauer, F. C. I. V. Pickard, A. C. Simmonett, W. D. Allen, E. Matyus, A. G. Csaszar, *Nature* **2008**, *453*, 906 – 909.
[15] J. Pranata, D. A. Dougherty, *J. Phys. Org. Chem.* **1989**, *2*, 161 – 176.
[16] M. B. Sponsler, R. Jain, F. D. Coms, D. A. Dougherty, *J. Am. Chem. Soc.* **1989**, *111*, 2240 – 2252.
[17] P. S. Zuev, R. S. Sheridan, T. V. Albu, D. G. Truhlar, D. A. Hrovat, W. T. Borden, *Science* **2003**, *299*, 867 – 870.
[18] R. A. Moss, R. R. Sauers, R. S. Sheridan, J. Tian, P. S. Zuev, *J. Am. Chem. Soc.* **2004**, *126*, 10196 – 10197.
[19] A. Datta, D. A. Hrovat, W. T. Borden, *J. Am. Chem. Soc.* **2008**, *130*, 6684 – 6685.
[20] O. M. Gonzalez-James, X. Zhang, A. Datta, D. A. Hrovat, W. T. Borden, D. A. Singleton, *J. Am. Chem. Soc.* **2010**, *132*, 12548 – 12549.
[21] P. Carsky, J. Michl, *Theor. Chim. Acta* **1992**, *84*, 125 – 133.
[22] H. Inui, K. Sawada, S. Oishi, K. Ushida, R. J. McMahon, *J. Am. Chem. Soc.* **2013**, *135*, 10246 – 10249.
[23] B. K. Carpenter, *J. Am. Chem. Soc.* **1983**, *105*, 1700 – 1701.
[24] B. R. Arnold, J. G. Radziszewski, A. Campion, S. S. Perry, J. Michl, *J. Am. Chem. Soc.* **1991**, *113*, 692 – 694.
[25] G. Maier, R. Wolf, H. O. Kalinowski, *Angew. Chem.* **1992**, *104*, 764 – 766.
[26] G. L. Snyder, D. A. Dougherty, *J. Am. Chem. Soc.* **1989**, *111*, 3942 – 3954.
[27] W. Sander, G. Bucher, F. Reichel, D. Cremer, *J. Am. Chem. Soc.* **1991**, *113*, 5311 – 5322.
[28] D. C. Merrer, R. A. Moss, M. T. H. Liu, J. T. Banks, K. U. Ingold, *J. Org. Chem.* **1998**, *63*, 3010 – 3016.
[29] E. Kraka, D. Cremer, *J. Phys. Org. Chem.* **2002**, *15*, 431 – 447.
[30] E. M. Greer, C. V. Cosgriff, C. Doubleday, *J. Am. Chem. Soc.* **2013**, *135*, 10194 – 10197.
[31] M. Pettersson, E. M. S. Macoas, L. Khriachtchev, J. Lundell, R. Fausto, M. Rasanen, *J. Chem. Phys.* **2002**, *117*, 9095 – 9098.
[32] J. Sabelko, J. Ervin, M. Gruebele, *Proc. Natl. Acad. Sci. USA* **1999**, *96*, 6031 – 6036.
[33] P. L. Biancaniello, A. J. Kim, J. C. Crocker, *Biophys. J.* **2008**, *94*, 891 – 896.
[34] G. Bazsó, S. Gobi, G. Tarczay, *J. Phys. Chem. A* **2012**, *116*, 4823 – 4832.
[35] I. Reva, M. J. Nowak, L. Lapinski, R. Fausto, *J. Chem. Phys.* **2012**, *136*, 064511/064511 – 064511/064518.
[36] S. Lopes, A. V. Domanskaya, R. Fausto, M. Raesaenen, L. Khriachtchev, *J. Chem. Phys.* **2010**, *133*, 144507/144501 – 144507/144507.
[37] A. Sole, S. Olivella, J. M. Bofill, J. M. Anglada, *J. Phys. Chem.* **1995**, *99*, 5934 – 5944.
[38] W. Sander, R. Hubert, E. Kraka, J. Grafenstein, D. Cremer, *Chem-Eur J* **2000**, *6*, 4567 – 4579.
[39] B. Chen, A. Y. Rogachev, D. A. Hrovat, R. Hoffmann, W. T. Borden, *J. Am. Chem. Soc.* **2013**, *135*, 13954 – 13964.
[40] K. Andersson, P. A. Malmqvist, B. O. Roos, *J. Chem. Phys.* **1992**, *96*, 1218 – 1226.
[41] D. G. Truhlar, B. C. Garrett, *Annu. Rev. Phys. Chem.* **1984**, *35*, 159 – 189.
[42] A. E. Fernandez-Ramos, B. C. Garrett, D. G. Truhlar, in *Reviews in Computational Chemistry*, John Wiley & Sons, Inc., **2007**, pp. 125 – 232.
[43] S. Kozuch, X. Zhang, D. A. Hrovat, W. T. Borden, *J. Am. Chem. Soc.*, **2013**, *135*, 17274 – 17277.
[44] Y. Y. Chuang, J. C. Corchado, D. G. Truhlar, *J. Phys. Chem. A* **1999**, *103*, 1140 – 1149.
[45] T. H. Dunning, *J. Chem. Phys.* **1989**, *90*, 1007 – 1023.
[46] R. A. Kendall, T. H. Dunning Jr., R. J. Harrison, *J. Chem. Phys.* **1992**, *96*, 6796 – 6806.

[47] POLYRATE - Version 2008, J. Zheng, S. Zhang, B. J. Lynch, J. C. Corchado, Y.-Y. Chuang, P. L. Fast, W.-P. Hu, Y.-P. Liu, G. C. Lynch, K. A. Nguyen, C. F. Jackels, A. Fernandez-Ramos, B. A. Ellingson, V. S. Melissas, J. Villa, I. Rossi, E. L. Coitino, J. Pu, T. V. Albu, R. Steckler, B. C. Garrett, A. D. Isaacson, D. G. Truhlar, University of Minnesota, Minneapolis, MN, **2009**.

[48] Gaussian 09, M. J. T. Frisch, G. W.; Schlegel, H. B.; Scuseria, G. E.; Robb, M. A.; Cheeseman, J. R.; Scalmani, G.; Barone, V.; Mennucci, B.; Petersson, G. A.; Nakatsuji, H.; Caricato, M.; Li, X.; Hratchian, H. P.; Izmaylov, A. F.; Bloino, J.; Zheng, G.; Sonnenberg, J. L.; Hada, M.; Ehara, M.; Toyota, K.; Fukuda, R.; Hasegawa, J.; Ishida, M.; Nakajima, T.; Honda, Y.; Kitao, O.; Nakai, H.; Vreven, T.; Montgomery, Jr., J. A.; Peralta, J. E.; Ogliaro, F.; Bearpark, M.; Heyd, J. J.; Brothers, E.; Kudin, K. N.; Staroverov, V. N.; Kobayashi, R.; Normand, J.; Raghavachari, K.; Rendell, A.; Burant, J. C.; Iyengar, S. S.; Tomasi, J.; Cossi, M.; Rega, N.; Millam, N. J.; Klene, M.; Knox, J. E.; Cross, J. B.; Bakken, V.; Adamo, C.; Jaramillo, J.; Gomperts, R.; Stratmann, R. E.; Yazyev, O.; Austin, A. J.; Cammi, R.; Pomelli, C.; Ochterski, J. W.; Martin, R. L.; Morokuma, K.; Zakrzewski, V. G.; Voth, G. A.; Salvador, P.; Dannenberg, J. J.; Dapprich, S.; Daniels, A. D.; Farkas, Ö.; Foresman, J. B.; Ortiz, J. V.; Cioslowski, J.; Fox, D. J., Gaussian, Inc., Wallingford CT, **2009**.

[49] GAUSSRATE - Version 2009, J. Zheng, S. Zhang, J. C. Corchado, Y.-Y. Chuang, E. L. Coitino, B. A. Ellingson, D. G. Truhlar, University of Minnesota, Minneapolis, MN, **2009**.

[50] MOLCAS Version 7.4, G. Karlström, R. Lindh, P.-Å. Malmqvist, B. O. Roos, U. Ryde, V. Veryazov, P.-O. Widmark, M. Cossi, B. Schimmelpfennig, P. Neogrady, L. Seijo, *Comput. Mater. Sci.* **2003**, *28*, 222 – 239.

[51] R. P. Bell, *The Tunnel Effect in Chemistry*, Chapman and Hall, London, **1980**.

[52] R. S. Sheridan, in *Reviews of Reactive Intermediate Chemistry* (Ed.: M. S. M. Platz, R. A.; Jones, M., Jr.), John Wiley & Sons, New York, **2007**, pp. 415 – 463.

[53] D. Ley, D. Gerbig, P. R. Schreiner, *Org. Biomol. Chem.* **2012**, *10*, 3781 – 3790.

Received: September 27, 2013
Published online on ■■ ▮▮, 0000

FULL PAPER

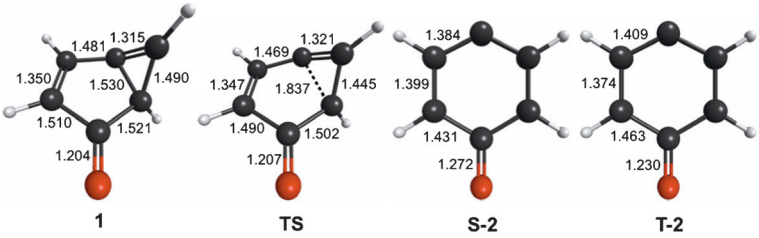

Quantum mechanical tunneling: Despite an estimated activation barrier of more than 6 kcal mol^{-1}, the strained cyclopropene **1** rearranges at temperatures as low as 3 K to the carbene **2** in its triplet ground state (see figure). Experiments and theory provide clear evidence that the rearrangement proceeds through heavy-atom tunneling.

Rearrangement Reactions

*M. Ertelt, D. A. Hrovat, W. T. Borden, W. Sander**

■■ – ■■

Heavy-Atom Tunneling in the Ring Opening of a Strained Cyclopropene at Very Low Temperatures